11^{th} World Congress on Structural and Multidisciplinary Optimization
7^{th} - 12^{th}, June 2015, Sydney Australia

Optimization of contact stress distribution in interference fit

Niels Leergaard Pedersen

Dept. of Mechanical Engineering, Solid Mechanics, Technical University of Denmark
Nils Koppels Allé, Building 404, DK-2800 Kgs. Lyngby, Denmark
email: nlp@mek.dtu.dk

1. Abstract
Assembly of shaft and hub by an interference fit is a classical connection with known advantages and disadvantages. The advantage being the level of possible torque transfer while the disadvantage is a possible fretting fatigue failure at the points of stress concentration. The pressure distribution in the contact is the source responsible for the fatigue failure. The distribution can be improved by design modification done directly on the contacting surfaces which however requires a very high production precision. Alternatively it is shown, how shape optimization of the hub side can improve the pressure distribution significantly.

2. Keywords: Interference fit, Contact, Optimization, Stress concentration.

3. Introduction
Interference fit or press fit is one of the most used assembly methods for shaft-hub connections. This type of assembly is superior with respect to possible torque transmission between two assembled parts. The disadvantage is that in the typical configuration disassembly is not possible. The limit to the used of an interference fit is typically dictated by the maximum heating or cooling of the parts during the assembly process. Once assembled the interference fit may fail due to fretting fatigue. Fretting fatigue is a type of fatigue where the parts due to relative movement between compressed parts fail. The failure is a gradual deterioration of the surface resulting in loss of contact pressure.

In a traditional design with straight assembly surfaces for shaft and hub, the result is a large stress concentration at the end of contact. The shaft is in the working condition typically loaded in both bending and torsion. The combination of the high stress and the relative motion result in the fretting fatigue. Results from roller bearings, see [1] and [2] indicate that for this case, although not directly comparable, is possible to achieve a constant contact pressure by special design of the rollers. Design changes to the interference fit contact surfaces should therefore also be possible. In the literature many different design changes have been proposed for improving the strength of the interference fit, different ways of changing the contact can be found in e.g. [3], [4], [5], [6], [7] and [8]. Improving the interference design by shape changes made to the hub can be found in [3] and [9]. For most of the papers the design improvement has been done without a focus directly on optimization but more by a trial an error method.

It might not be straight forward What the shape of an optimal contact pressure should be. If fretting fatigue is to be avoided then there should be no relative motion between the two parts in contact, the possibility for relative motion is controlled by the friction coefficient and the normal pressure, therefore one could argue that the contact pressure at the inlet to the contact should be high. This reasoning have lead to suggested design improvement where, e.g., there is a groove in the shaft and the hub has an overhang over part of this groove leading to an even higher stress concentration at the contact inlet. On the other hand if there is relative motion between two parts in contact then the contact pressure should be low in order not to result in fretting fatigue. As seen in the paper [10] the high stress values can result in deterioration of either the hub or the shaft or both due to the high stress. The interference fit should function in situations where the connection typically is loaded both in bending and torsion. The torsion only creates shear motion and therefore for a pure torsional load of an interference fit the way to design the contact pressure is one where the contact pressure is so high that relative motion is avoided and at the same time no deterioration of the surfaces takes place due to plasticity. For the interference fit in bending (rotating) it seems that even though the stresses are high at the inlet the stress will either be increased to a too high level or there will be inherently a relative motion between the two part. The design objective for the present work is therefore to have a constant contact pressure between the parts. The level of this contact pressure should be selected such that the fretting fatigue is avoided on one hand and on the other hand so high as possible to fully take advantage of the interference fit.

4. Stress singularity of standard design

To evaluate the size of the stress singularity a FE model with a mesh refinement is needed. Reducing the element size at the singularity will increase the maximum stress and the size of the stress will go to infinity as the element size goes towards zero.

The data for the shaft and hub connection used in the present work is

- Shaft: length $L_s = 0.6$m, diameter $D_f = 0.2$m
- Hub: Length $L_h = 0.3$m, thickness $t = 0.1$m , i.e., outer diameter of hub $D_h = 0.4$m

The interference is introduced in the finite element model by modeling a cooling of the hub by 100°C. The material properties of the hub and shaft are assumed identical and given by

$$E = 2.1 \cdot 10^5 \text{MPa}, \qquad \nu = 0.3, \qquad \alpha = 1.1 \cdot 10^{-5}/^\circ\text{C}$$

where E is modulus of elasticity, ν is Poisson's ratio and α is the thermal expansion coefficient. A cooling of the hub by 100°C is used and this results in an interference fit of $\delta_d = 220\mu$m. The classical analytical pressure in the connection, under the assumption of rotational symmetry and infinitely long shaft and hub (plane model), is given by

$$p_f = \frac{E\delta_d}{2D_f}\left(1 - \left(\frac{D_f}{D_h}\right)^2\right) \tag{1}$$

where $D_h = D_F + 2 \cdot t$ is the outer diameter of the hub. With the given data the pressure is $p_f = 86.6$MPa. The size of the singularity for the present design is estimated using the COMSOL program ([11]). The connection is modeled assuming axis symmetry as seen in Figure 2. In the contact modeling it is examined if the inclusion of friction is important for the evaluation of the pressure, from the computation it is found that the friction does have an influence but that it has an negligible influence on the contact pressure.

In order to evaluate the stress concentration factor it is here selected to identify the stress 10μm from the edge of the hub. The overall distribution of the stress is given in Figure 1a) and in Figure 1b) a zoom of the last 1mm is shown. The finite element model is highly refined with 30 FE nodes along the last 10μm of the contact in 1a) and in the shown zoom with 60 FE nodes along the last 10μm. The stress converges to a level of 415MPa. From the computation we conclude that the theoretical stress concentration K_t for this case is

$$K_t \approx \frac{415}{86.6} = 4.8 \tag{2}$$

The exact value of the theoretical stress concentration factor can always be discussed. But it is clear that the stress concentration has a significant size.

5. Super element technique for contact analysis

An alternative to performing contact analysis by a traditional iterative finite element analysis (FEA) is to use the super element technique. The procedure involves no iterations see [12]. Application of the method for shrink fit analysis can be found in [13] and in relation to bolted connection see [14]. The primary advantage of the method is that no iterations are needed in the FE calculation. In Figure 2 an interference fit is shown. The axis symmetric model of half the connection is also shown together with the contact pressure distribution.

In the analysis the shaft and hub are separated. The super element FE model of the hub alone is given as

$$[S_{hp}]\{D_{hp}\} = \{F_{cp}\} \tag{3}$$

where $[S_{hp}]$ is the hub super element stiffness matrix. The order of this matrix equals the number of FE mesh nodes on the contact line. The resulting displacements of the contacting nodes are $\{D_{hp}\}$ and the corresponding nodal contact pressure forces are $\{F_{cp}\}$. The total contacting force is given as the sum of these nodal forces i.e.

$$F_p = ||\{F_{cp}\}||_1 \tag{4}$$

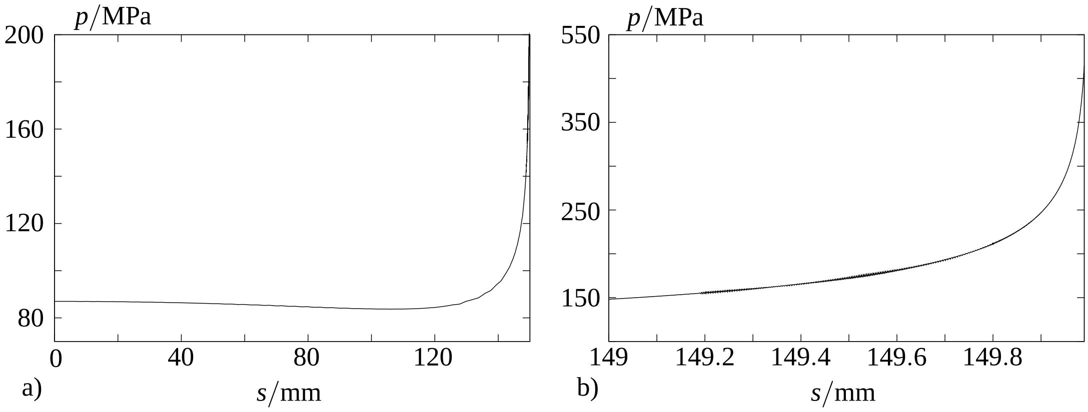

Figure 1: Contact pressure along interference fit. a) Full length of contact. b) Zoom of last 1mm of contact, the stress is not plotted for the last 10μm due to the singularity, the maximum stress 10μm from the edge is 415MPa.

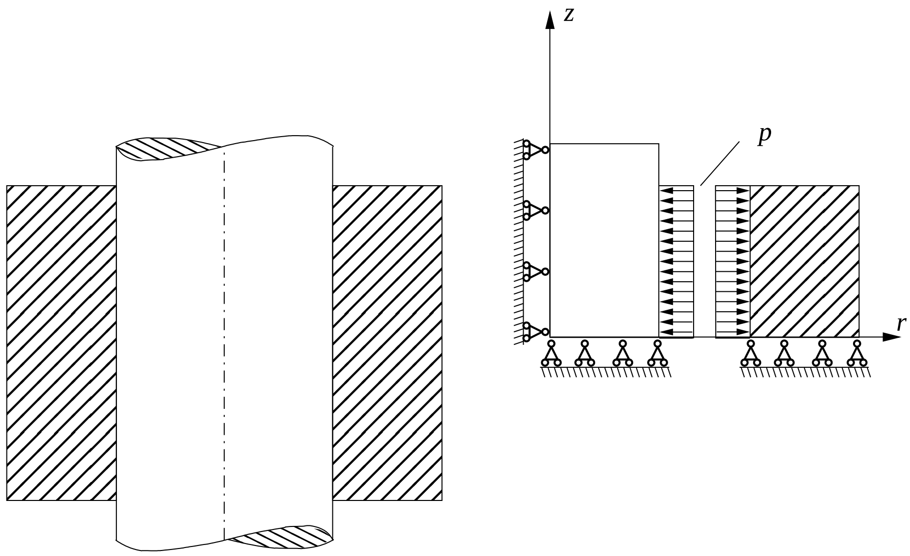

Figure 2: left: the interference fit. Right: of this an illustration of the axis symmetric model of half the shaft and hub used in the analysis. The contact pressure p is illustrated by a distribution that it is to be determined from the analysis.

With respect to the practical determination of the super element matrices see [12].

It is assumed that the contact line on the shaft has the same number of nodes (mutual corresponding) as the hub contact line. The analysis for the shaft can under this assumption be performed in a similar manner using the super finite element matrices for this part.

$$[S_{sp}]\{D_{sp}\} = -\{F_{cp}\} \tag{5}$$

where $[S_{sp}]$ is the shaft super element stiffness matrix. The order of this matrix also equals the number of FE mesh nodes on the contact line. The resulting displacements of the contacting nodes are $\{D_{sp}\}$ and the corresponding nodal contact pressure forces are $-\{F_{cp}\}$, i.e., a negative sign relative to the analysis of the hub, to express equilibrium with (3),

Before assembly the radial interference (negative gap) between the shaft and hub for the nodes on the line of contacts can be determined as

$$\{g\} = \{r_s\} - \{r_h\} \tag{6}$$

where $\{r_s\}$ and $\{r_h\}$ are the radial position of the nodes on the contact line for the shaft and hub respectively. After the two components are fitted together the nodes will be at the same point, i.e. we have that

$$\{r_s\} + \{D_{sp}\} = \{r_h\} + \{D_{sh}\} \Rightarrow \{g\} = \{D_{sh}\} - \{D_{sp}\} \tag{7}$$

The super element technique can be used in two different ways; either the contact force distribution, $\{F_{cp}\}$, is assumed known and from this the gap, $\{g\}$, can be found directly by

$$\{g\} = ([S_{hp}]^{-1} + [S_{sp}]^{-1})\{F_{cp}\} \tag{8}$$

alternatively the gap is assumed known and the contact force can be found from

$$\{F_{cp}\} = ([S_{hp}]^{-1} + [S_{sp}]^{-1})^{-1}\{g\} \tag{9}$$

The result we achieve is that under the given assumptions then contact force can be found directly without iterations from a given gap distribution. The analysis involved the determination of the inverse matrices for the two super finite element stiffness matrices, but the size of these is limited to the number of nodes on the contact line.

6. Design modification of contact zone

Under the assumption used in (8) we may find the gap $\delta(z)$, as a function of the position z, that will result in a constant stress. In Figure 3 the resulting gap for the shaft hub design used in the present work with a constant pressure of 86.6MPa is shown.

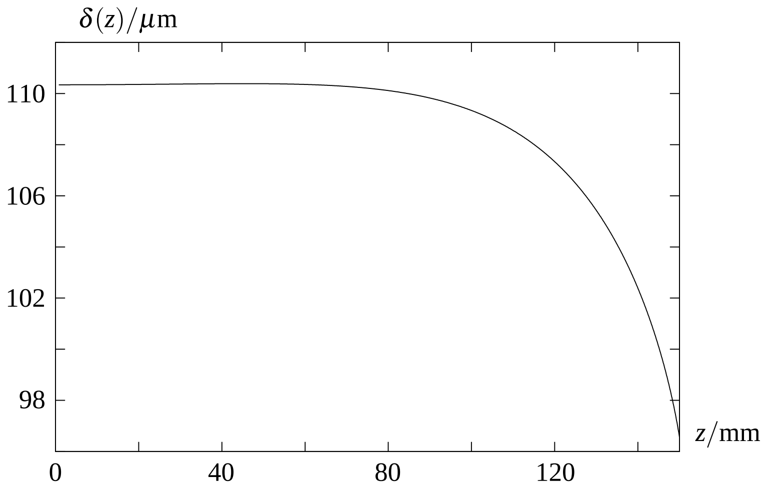

Figure 3: Gap as a function of axial position (see Figure 2) that result in a constant pressure, 86.6MPa, in the interference fit.

As can be seen in Figure 3 the variation in the gap is not very high as compared to the normal production methods where the interference is specified by tolerances, the variation lies in this case within 14μm. Creating a shaft and hub with exactly the shown interference is therefore not desirable.

The results indicates that the connection for a constant interference is to stiff at the run-out of the hub relative to achieve a constant contact pressure. One way of changing this assuming that a constant interference is used is to make design changes to the hub side. A simple design change is to make a chamfer of the hub as seen in Figure 4a). The optimization problem can be stated as minimize the variation in the gap for a given constant pressure. The optimal design for this design change is shown in Figure 4b). The given simple design parameterization does not allow for a completely constant gap.

In Figure 4b) the optimal value of the chamfer is $a = 15.5$mm which gives a total variation in the interference of 3.5μm to be compared to the original 14μm for no chamfer $a = 0$mm.

One disadvantage of the presented chamfer design is the reduction in the possible use of the hub, e.g., we can not use the whole length for a gear.

Alternative design change will be presented in the lecture. also the application of traditional contact analysis will be shown.

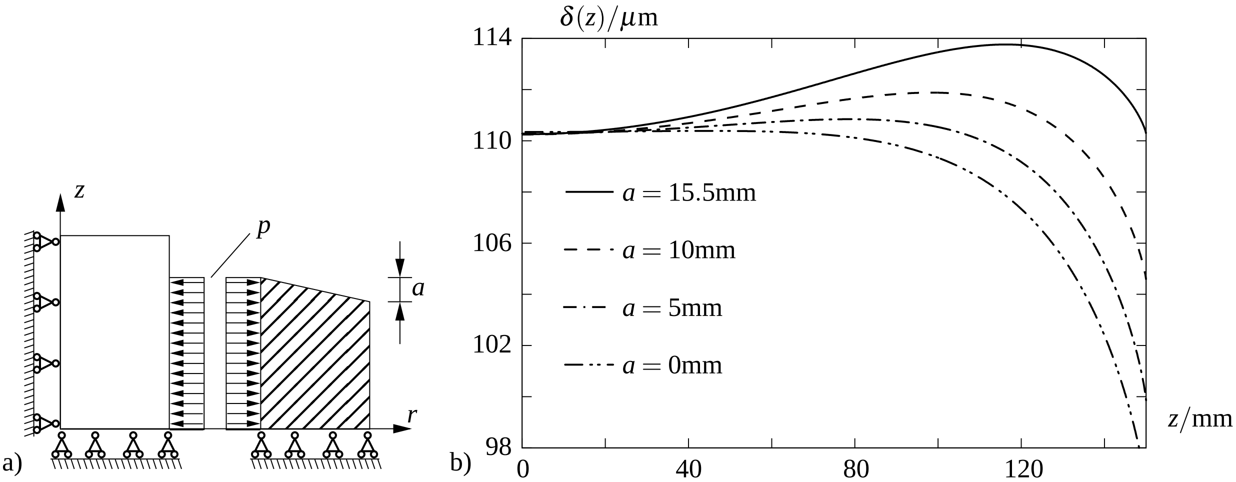

Figure 4: Gap as a function of axial position for different chamfer size that result in a constant pressure, 86.6MPa, in the interference fit.

7. References

[1] H. Reusner. The logarithmic roller profile - the key to superior performance of cylindrical and taper roller bearings. *Ball bearing journal*, 230:2–10, 1987.

[2] H. Fujiwara and T. Kawase. Logarithmic profiles of rollers in roller bearings and optimization of the profiles (reprint from the original paper (in Japanese) from the proceedings of the japan society of mechanical engineers part c, vol 72 (2006),3022-2029). *NTN Technical review*, 70:140–148, 2007.

[3] K. Nishioka and H. Komatsu. Researches on increasing the fatigue strength of press-fitted shaft assembly. *Bulletin of the Japan Society of Mechanical Engineers*, 10(42):880–889, 1967.

[4] D. J. White and J. Humpherson. Finite-element analysis of stresses in shafts due to interference-fit hubs. *Journal of Strain Analysis for Engineering Design*, 4(2):105–114, 1969.

[5] Toshio Hattori, Sueo Kawai, Noriaki Okamoto, and Tadashi Sonobe. Torsional fatigue strength of a shrink fitted shaft. *Bulletin of the JSME*, 24(197):1893–1900, 1981.

[6] Dong Hyong Lee, Seok Jin Kwon, Jeong Won Seo, and Won Hee You. Effects of hub contact shape on contact pressure and fatigue life in a press-fitted shaft. *Materials Science Forum, Mater. Sci. Forum*, 654-656:1638–1641, 2010.

[7] Shunsuke Kataoka, Chu Sakae, Masanobu Kubota, and Yoshiyuki Kondo. Effect of stress relief groove shape on fretting fatigue strength. *Key Engineering Materials*, 353-358(PART 2):856–859, 2007.

[8] Guillaume Biron, Aurelian Vadean, and Lucian Tudose. Optimal design of interference fit assemblies subjected to fatigue loads. *Structural and multidisciplinary optimization*, 47(3):441–451, 2013.

[9] T. Juuma. Torsional fretting fatigue strength of a shrink-fitted shaft with a grooved hub. *Tribology international*, 33(8):537–543, 2000.

[10] Masanobu Kubota, Shunsuke Kataoka, and Yoshiyuki Kondo. Effect of stress relief groove on fretting fatigue strength and index for the selection of optimal groove shape. *International journal of fatigue*, 31(3):439–446, 2009.

[11] COMSOL AB. Stockholm, www.comsol.se, 1998-2009.

[12] P. Pedersen. A direct analysis of elastic contact using super elements. *Computational mechanics*, 37(3):221–231, 2006.

[13] Pauli Pedersen. On shrink fit analysis and design. *Computational Mechanics*, 37(2):121–130, 2006.

[14] Niels Leergaard Pedersen and Pauli Pedersen. Bolt-plate contact assemblies with prestress and external loads: Solved with super element technique. *Computers and Structures*, 87(21-22):1374–1383, 2009.